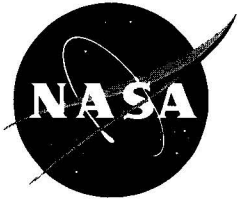


NASA Contractor Report NASA/CR-2008-214744



Impact of Local Sensors

Leela R. Watson
William H. Bauman III
*Applied Meteorology Unit
Kennedy Space Center, Florida*

June 2008

NASA STI Program ... in Profile

Since its founding, NASA has been dedicated to the advancement of aeronautics and space science. The NASA scientific and technical information (STI) program plays a key part in helping NASA maintain this important role.

The NASA STI program operates under the auspices of the Agency Chief Information Officer. It collects, organizes, provides for archiving, and disseminates NASA's STI. The NASA STI program provides access to the NASA Aeronautics and Space Database and its public interface, the NASA Technical Report Server, thus providing one of the largest collections of aeronautical and space science STI in the world. Results are published in both non-NASA channels and by NASA in the NASA STI Report Series, which includes the following report types:

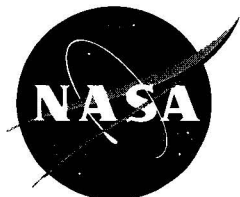
- **TECHNICAL PUBLICATION.** Reports of completed research or a major significant phase of research that present the results of NASA Programs and include extensive data or theoretical analysis. Includes compilations of significant scientific and technical data and information deemed to be of continuing reference value. NASA counterpart of peer-reviewed formal professional papers but has less stringent limitations on manuscript length and extent of graphic presentations.
- **TECHNICAL MEMORANDUM.** Scientific and technical findings that are preliminary or of specialized interest, e.g., quick release reports, working papers, and bibliographies that contain minimal annotation. Does not contain extensive analysis.
- **CONTRACTOR REPORT.** Scientific and technical findings by NASA-sponsored contractors and grantees.
- **CONFERENCE PUBLICATION.** Collected papers from scientific and technical conferences, symposia, seminars, or other meetings sponsored or co-sponsored by NASA.
- **SPECIAL PUBLICATION.** Scientific, technical, or historical information from NASA programs, projects, and missions, often concerned with subjects having substantial public interest.
- **TECHNICAL TRANSLATION.** English-language translations of foreign scientific and technical material pertinent to NASA's mission.

Specialized services also include creating custom thesauri, building customized databases, and organizing and publishing research results.

For more information about the NASA STI program, see the following:

- Access the NASA STI program home page at <http://www.sti.nasa.gov>
- E-mail your question via the Internet to help@sti.nasa.gov
- Fax your question to the NASA STI Help Desk at (301) 621-0134
- Phone the NASA STI Help Desk at (301) 621-0390
- Write to:
NASA STI Help Desk
NASA Center for AeroSpace Information
7121 Standard Drive
Hanover, MD 21076-1320

NASA Contractor Report NASA/CR-2008-214744



Impact of Local Sensors

Leela R. Watson
William H. Bauman III
Applied Meteorology Unit
Kennedy Space Center, Florida

June 2008

Acknowledgements

The authors thank Mr. William Roeder of the 45th Weather Squadron for his guidance on the methodology used to select cases, his independent review of the differing model forecasts with different initializing data from the operational perspective, and for his suggestion to conduct an objective analysis of the data for this task.

Available from:

NASA Center for AeroSpace Information
7121 Standard Drive
Hanover, MD 21076-1320
(301) 621-0390

This report is also available in electronic form at

<http://science.ksc.nasa.gov/amu/>

Executive Summary

Forecasters at the 45th Weather Squadron (45 WS) use observations from the Kennedy Space Center (KSC) and Cape Canaveral Air Force Station (CCAFS) wind tower network and the CCAFS (XMR) daily rawinsonde observations (RAOB) to issue and verify wind advisories and warnings for operations. These observations are also used by the National Weather Service (NWS) Spaceflight Meteorology Group (SMG) in Houston, Texas and the NWS Melbourne, Florida (NWS MLB) to initialize their locally run mesoscale models. SMG also uses them to support shuttle landings at the KSC Shuttle Landing Facility (SLF). Due to impending budget cuts, some or all of the KSC/CCAFS wind towers on the east-central Florida mainland and all but one of the daily XMR RAOBs may be eliminated. The loss of these data may impact the forecast capability of the 45 WS, SMG and NWS MLB.

The Applied Meteorology Unit (AMU) was tasked to conduct a modeling study to determine how important these observations are to the accuracy of the model which is being used as a proxy for the utility of these observations in general forecasting to the 45 WS forecasters. To accomplish this, the AMU performed a sensitivity study using the Weather Research and Forecasting (WRF) model initialized with and without KSC/CCAFS wind tower and XMR RAOB observations. The AMU assessed the accuracy of model output by comparing peak wind forecasts with observed winds based on operationally significant wind advisories and warnings issued by the 45 WS to determine if the model could aid in the issuance of the advisories and warnings. To assess model performance when initialized with and without some of the wind tower and XMR RAOB observations, the AMU conducted subjective and objective analyses. In the subjective analysis, the model wind forecasts were displayed graphically with the observations overlaid for comparison. In the objective analysis, the maximum peak wind forecast was compared to the maximum peak wind observed within the KSC/CCAFS wind tower network.

The AMU collected data for 12 warm season cases from June – September 2007 and eight cool season cases from November – January 2008. For each case chosen, the 45 WS must have issued a wind advisory or warning for the KSC/CCAFS area and the KSC/CCAFS wind towers must have recorded significant wind events, or winds greater than 18 kt. These criteria would determine if the model could aid in the forecasters issuance of wind advisories and warnings.

The model configuration used a “hot-start” initialization of the Weather Research and Forecasting (WRF) model using the Local Analysis and Prediction System (LAPS). Each run started at 0900 UTC and was integrated 12 hours with a 1.3 km horizontal grid spacing and 40 irregularly spaced, vertical sigma levels, with a greater number of levels located in the planetary boundary layer. LAPS was initialized with Level II Weather Surveillance Radar-1988 Doppler (WSR-88D) data from the Melbourne, Florida radar, Geostationary Operational Environmental Satellites (GOES) visible and infrared satellite imagery, Meteorological Assimilation Data Ingest System (MADIS) data, and KSC/CCAFS wind tower data and the XMR RAOB. The AMU initialized WRF under four different initialization scenarios:

- With the mainland towers and without the 1000 UTC XMR RAOB,
- With the mainland towers and with the 1000 UTC XMR RAOB,
- Without the mainland towers and without the 1000 UTC XMR RAOB, and
- Without the mainland towers and with the 1000 UTC XMR RAOB.

The AMU completed the subjective analysis of the WRF forecasts by comparing model output to observations at the time of the maximum peak wind corresponding to the 45 WS advisories and warnings for that day to determine if any of the four scenarios produced better results than the others.

For the objective analysis, the AMU identified model-domain maximum peak wind speeds for each forecast output time and compared them to the observed maximum peak wind speed in the domain. An overall evaluation of how well the four model scenarios performed against each other was then conducted.

In both the subjective and objective analyses, there was minimal difference among the four WRF model scenarios. The WRF model performed better in the cool season during prevailing synoptic forcing regimes. The model also proved to be a good indicator of the threat of advisory or warning criteria wind speeds over each 12-hr forecast model run. This would provide added value to the forecaster’s daily planning forecast.

Table of Contents

Executive Summary	4
List of Figures	6
List of Tables.....	7
1. Introduction.....	8
2. Data and Model Configuration.....	10
2.1 Determining Warm and Cool Season Candidate Days.....	10
2.2 WRF-ARW Model and LAPS Initialization.....	10
2.3 Data Ingest.....	11
2.4 Model Configuration	12
2.5 Problems Encountered.....	13
3. Analyses	14
3.1 Subjective Wind Analysis	14
3.1.1 Warm Season.....	14
3.1.2 Cool Season.....	16
3.2 Objective Peak Wind Analysis	18
4. Summary and Conclusions.....	24
References	25
List of Acronyms.....	26

List of Figures

Figure 1.	The KSC/CCAFS wind tower network. Locations with a magenta triangle represent the mainland towers that may be eliminated and were removed from the some of the model initializations. The XMR RAOB site is located at the red triangle.	8
Figure 2.	Map of east-central Florida showing the model domain boundary (gray square) and distribution of surface observations. The legend indicating the observation type is located at the top right of the figure. County names are light gray and the KSC and CCAFS labels are black.	12
Figure 3.	Comparison of the 2100 UTC model forecast radar reflectivity (contours) to the 2117 UTC observed radar reflectivity from the NWS MLB WSR-88D (shaded) for the four scenarios on 20 June 2007. The model forecast radar reflectivity contours based on (a) the mainland towers and no RAOB , (b) mainland towers with the RAOB , (c) no mainland towers and no RAOB and (d) no mainland towers with RAOB . The reflectivity scale (dBZ) is shown at the top of each map. The location of the maximum peak wind speed is shown at Tower 421 by the red dot. The approximate broken line of observed convection is shown in blue.	15
Figure 4.	Comparison of the 2100 UTC model forecast peak winds (shaded) to the 2115 UTC wind tower observations for the four scenarios of data withholding on 20 June 2007. The wind tower observations show the 5 minute average wind speed and direction (wind barb) and peak speed (number at upper right of the wind barb). The model forecast peak wind speeds based on the (a) mainland towers and no RAOB , (b) mainland towers with the RAOB , (c) no mainland towers and no RAOB and (d) no mainland towers with RAOB . The model wind speed scale (kt) is shown at the top of each map. The location of the maximum peak wind speed is shown at Tower 421 by the red circle.	16
Figure 5.	Comparison of the model forecast peak winds (shaded) to the wind tower observations for the four scenarios of data withholding on 17 January 2008 at 1500 UTC. The wind tower observations show the 5 minute average wind speed and direction (wind barb) and peak speed (number at upper right of the wind barb). The model forecast peak wind speeds based on the (a) mainland towers and no RAOB , (b) mainland towers with the RAOB , (c) no mainland towers and no RAOB and (d) no mainland towers with RAOB . The model wind speed scale (kt) is shown at the top of each map. The location of the maximum peak wind speed is shown at Tower 313 by the red circle.....	17
Figure 6.	Comparison of the model forecast average winds (shaded) to the wind tower observations for the four scenarios of data withholding on 17 January 2008 at 1500 UTC. The model forecast average wind speeds based on the(a) mainland towers and no RAOB , (b) mainland towers with the RAOB, (c) no mainland towers and no RAOB and (d) no mainland towers with RAOB . The black numbers are the 5 minute average wind speed observations at 54 ft. The location of the highest average wind speed is shown at Tower 313 by the red circle.The model wind speed scale (kt) is shown at the top of each map.	18
Figure 7.	Map of east-central Florida showing the location of the model sub-domain, outlined by the red-dashed rectangle, used in the objective analysis portion of this task.	19
Figure 8.	Chart of the observed maximum wind speed from the KSC/CCAFS towers and the model forecast maximum peak wind speed for the four scenarios on 11 July 2007 for all 12 1-hour forecast periods.	20
Figure 9.	Chart of the observed maximum wind speed from the KSC/CCAFS towers and the model forecast maximum peak wind speed for the four scenarios on 17 January 2008 for all 24 30-minute forecast periods.	20
Figure 10.	Chart showing the differences in WRF forecasts of maximum peak wind speed among the four scenarios for each hour of the model forecast for both the warm season (red line) and cool season (blue line).	22
Figure 11.	Chart showing the RMSE among the four WRF forecasts of maximum peak wind speed and the observations for each hour of the model forecast for both the warm season (red line) and cool season (blue line).	23

List of Tables

Table 1.	List of the all candidate days and observed maximum peak wind speed recorded for the day.	10
Table 2.	List of the physics options used for each LAPS-WRF model run.	13
Table 3.	Differences in the WRF maximum peak wind speed forecasts among the four “with and without” data scenarios for all of the warm season and cool season cases for each forecast hour of the model.	21
Table 4.	The MSE of the WRF maximum peak wind speed forecasts among the four “with and without” data scenarios compared to the observations for all of the warm season and cool season cases for each forecast hour of the model.	23

1. Introduction

Forecasters at the 45th Weather Squadron (45 WS) use observations from the Kennedy Space Center (KSC) and Cape Canaveral Air Force Station (CCAFS) wind tower network and the CCAFS (XMR) daily rawinsonde observations (RAOB) to issue and verify wind advisories and warnings for operations. These observations are also used by the National Weather Service (NWS) Spaceflight Meteorology Group (SMG) in Houston, Texas and the NWS Melbourne, Florida (NWS MLB) to initialize their locally-run mesoscale models. In addition, SMG uses these observations to support shuttle landings at the Shuttle Landing Facility (SLF). Due to impending budget cuts, some or all of the KSC/CCAFS wind towers on the east-central Florida mainland and the XMR RAOBs may be eliminated. The locations of the mainland towers and XMR RAOB site are shown in Figure 1. The loss of these data may impact the forecast capability of the 45 WS, SMG and NWS MLB. The AMU was tasked to conduct an objective independent modeling study to help determine how important these observations are to the accuracy of the model output used by the forecasters. To accomplish this, the Applied Meteorology Unit (AMU) performed a sensitivity study using the Weather Research and Forecasting (WRF) model initialized with and without KSC/CCAFS wind tower and XMR RAOB data.



Figure 1. The KSC/CCAFS wind tower network. Locations with a magenta triangle represent the mainland towers that may be eliminated and were removed from the some of the model initializations. The XMR RAOB site is located at the red triangle.

Twenty cases were chosen from data collected from June 2007 – January 2008. For each case chosen, the 45 WS must have issued a wind advisory or warning for the KSC/CCAFS area and the KSC/CCAFS wind towers must have recorded significant wind events, i.e. winds greater than 18 kt. This criteria would determine if the model could aid in the forecasters issuance of wind advisories and warnings. Due to the availability of background model data

used in the forecasts, a 0900 UTC model start time was chosen. This was the closest standard model initialization time to the 1000 UTC XMR RAOB which also allowed it to be included in the analysis. The AMU conducted model runs for each case using four different initialization scenarios:

- With the mainland towers and with the 1000 UTC XMR RAOB,
- With the mainland towers and without the 1000 UTC XMR RAOB,
- Without the mainland towers and with the 1000 UTC XMR RAOB.
- Without the mainland towers and without the 1000 UTC XMR RAOB, and

To assess model performance for each of the four runs, the AMU conducted subjective and objective analyses of the model wind forecasts comparing the maximum peak wind forecast to the maximum peak wind observed within the KSC/CCAFS wind tower network. This included conducting an evaluation of how the four model scenarios performed against each other to determine the effect the wind tower and RAOB data have on the model output. Also, the model output was compared to the observations to determine if any of the four scenarios produced better results than the others that could help the forecasters determine if wind advisories or warnings could be warranted during the next 12 hours.

2. Data and Model Configuration

The important aspects of this study were the choice of candidate warm and cool days, the model configuration, and the data used to initialize the models. The candidate warm season days were chosen over the June – September 2007 season and cool season days were chosen during November – January 2008.

2.1 Determining Warm and Cool Season Candidate Days

The period of record (POR) for choosing warm season candidate days was June through September 2007. At the request of the 45 WS, potential warm season candidate days had to meet three criteria. First, the 45 WS must have issued a wind advisory or warning for the KSC/CCAFS area. Next, days consisting of dominant synoptic-scale forcing patterns were eliminated from consideration. The AMU examined daily weather maps and used them to eliminate days in which there was a front or low pressure system over Florida or in the immediate area. Finally, the KSC/CCAFS wind towers must have recorded significant wind events, or winds greater than 18 kt. Twelve of the days in the POR met all three criteria (Table 1).

The POR for choosing cool season candidate days was November 2007 through January 2008. The two criteria for selection included the issuance of a wind advisory or warning for the KSC/CCAFS area by the 45 WS and the existence of specific cold season phenomena, such as fronts and their associated precipitation. Again, daily weather maps were examined to determine days in which there was a front or low pressure system over Florida or in the immediate area. Eight days in the POR met these criteria (Table 1).

Warm Season		Cool Season	
Candidate Day	Peak Wind (kt)	Candidate Day	Peak Wind (kt)
12 Jun 2007	40	11 Nov 2007	29
20 Jun 2007	38	16 Dec 2007	47
28 Jun 2007	33	21 Dec 2007	29
05 Jul 2007	25	03 Jan 2008	38
10 Jul 2007	28	17 Jan 2008	43
11 Jul 2007	35	20 Jan 2008	41
15 Jul 2007	35	25 Jan 2008	35
19 Jul 2007	34	27 Jan 2008	29
24 Jul 2007	45		
11 Sep 2007	23		
12 Sep 2007	27		
26 Sep 2007	32		

2.2 WRF-ARW Model and LAPS Initialization

The AMU employed the Weather Research and Forecasting (WRF) Model Environmental Modeling System (EMS) software, which was developed by the National Weather Service (NWS) Science Operations Officer (SOO) Science and Training Resource Center (STRC; <http://strc.comet.ucar.edu/wrf/index.htm>). A benefit of using the WRF EMS is that it incorporates both dynamical cores, Advanced Research WRF (ARW) and Non-hydrostatic Mesoscale Model (NMM), into a single end-to-end forecasting model (Rozumalski 2006). The software consists of pre-compiled programs that are easy to install and run.

For this task, the Advanced Research WRF (ARW) core was used. The ARW core was developed primarily at the National Center for Atmospheric Research (NCAR). It is a fully compressible, non-hydrostatic mesoscale model with a hydrostatic option. It consists of a mass-based hydrostatic pressure terrain following coordinate, Arakawa C-grid staggering for the horizontal grid, time-split integration using a third order Runge-Kutta scheme with a small step for acoustic and gravity wave modes, and up to sixth order advection options in the horizontal and vertical

(Skamarock et al. 2005). There are also full physics options for microphysics, planetary boundary layer, cumulus parameterization, radiation, and land surface schemes (Skamarock et al. 2005).

A “hot-start” initialization of the WRF model was made using the Local Analysis and Prediction System (LAPS; McGinley 1995). This analysis system allows the WRF model to benefit from the addition of high-resolution data sources in its initial conditions. LAPS is a data assimilation tool that uses numerous meteorological observations, such as satellite data, radar data, and surface observations, to generate a three-dimensional representation of the atmospheric forcing fields, such as wind speed and direction, surface temperature and pressure, relative humidity, precipitation and cloud cover (McGinley et al. 1991; Albers 1995; Albers et al. 1996; Birkenheuer 1999; McGinley 1995). LAPS includes a wind analysis and a three-dimensional cloud analysis, which are needed for the WRF hot-start initialization. The LAPS cloud analysis is designed to create consistency with all data and the typical meteorology of clouds by combining data from infrared and visible satellite data, three-dimensional LAPS radar reflectivity derived from the full volume radar data, and the LAPS three-dimensional temperatures (Albers et al. 1996). Fields derived from the cloud analysis include cloud liquid water, cloud type, cloud droplet size, and icing severity (Albers et al. 1996).

2.3 Data Ingest

Data ingested by the model through the LAPS analysis package included Level II Weather Surveillance Radar-1988 Doppler (WSR-88D) data from NWS MLB, Geostationary Operational Environmental Satellites (GOES) visible and infrared satellite imagery, Meteorological Assimilation Data Ingest System (MADIS; <http://madis.noaa.gov/>) data, and wind tower and XMR RAOB data. The Level II WSR-88D data contained full volume scans of reflectivity at a resolution of 1° by 1 km, radial velocity at 1° by 0.25 km, and spectrum width data at a 1° by 0.25 km (Fulton et al. 1998). These data were available every 4 to 6 minutes. The GOES-12 visible imagery was available at a 1 km horizontal resolution every 15 minutes, and the infrared imagery was available at a 4 km horizontal resolution also every 15 minutes. Both visible and infrared imagery provided brightness temperatures to the analysis packages.

Surface observation locations for hourly surface reports (METAR), buoys, MADIS and the KSC/CCAFS towers are shown in Figure 2. The MADIS data sets available for use in this task included mesonet, hydrological surface and multi-agency profiler data. Measured variables include surface wind and vertical wind profiles, temperature, dewpoint temperature, relative humidity, accumulated precipitation, etc., as well as types of weather occurrences such as hail, fog, and thunder. Local KSC/CCAFS tower data (Figure 1) used in the LAPS analysis included average wind speed and direction, peak speed and direction, temperature, dewpoint temperature, and relative humidity. The daily XMR 1000 UTC RAOB was also included in the LAPS analysis and its location is shown in Figure 1.

This task compared four LAPS data ingest combinations. These included all available data described above, all available data except mainland wind tower data, all available data except RAOB data, and all available data except mainland wind tower and RAOB data. These combinations were chosen to address possible model forecast degradation due to denial of local observations that may be lost due to budget cuts.

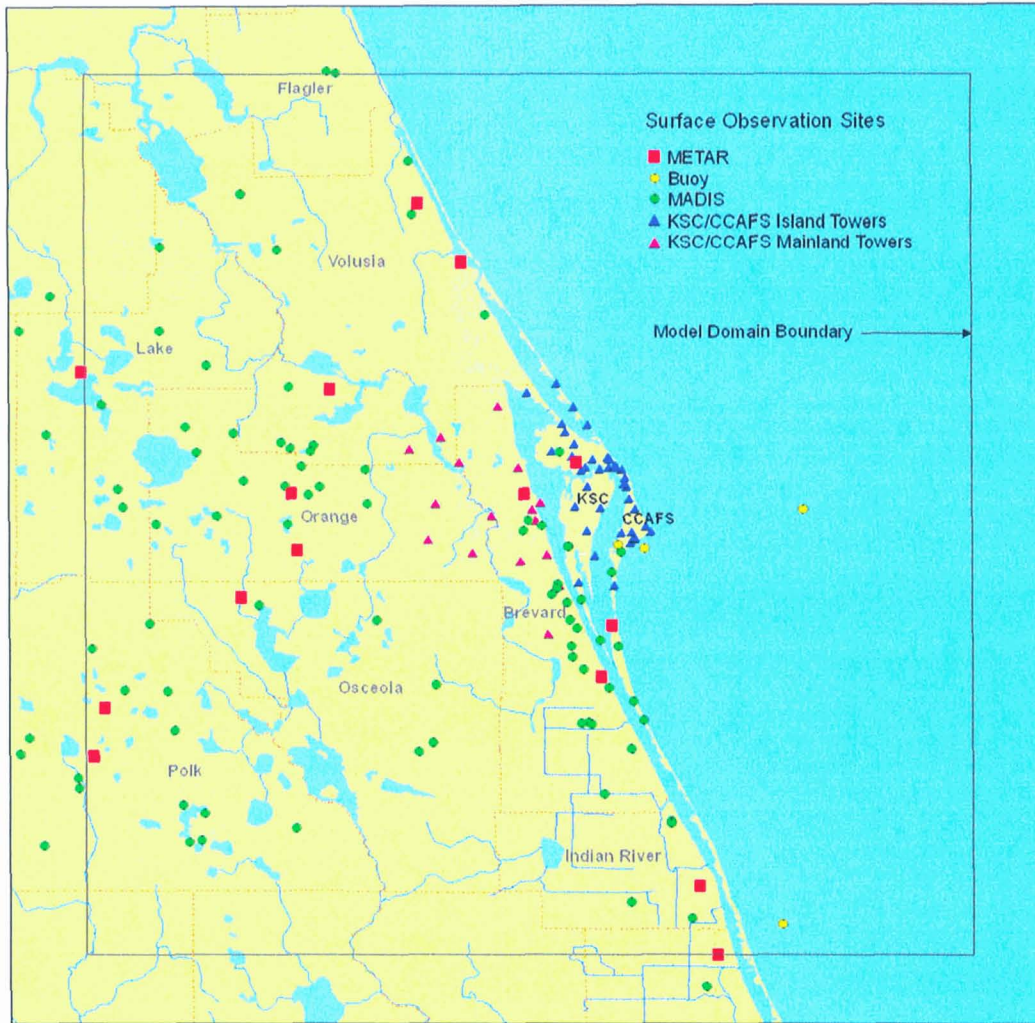


Figure 2. Map of east-central Florida showing the model domain boundary (gray square) and distribution of surface observations. The legend indicating the observation type is located at the top right of the figure. County names are light gray and the KSC and CCAFS labels are black.

2.4 Model Configuration

Each model simulation was run at a 1.3 km horizontal grid spacing centered over the KSC/CCAFS area with 40 irregularly spaced, vertical sigma levels. Each run started at 0900 UTC and was integrated 12 hours. A 0900 UTC initialization time was chosen as it was the closest standard model initialization time to the 1000 UTC XMR RAOB. There were four runs per day, one each for the four data denial configurations. The AMU evaluated 20 cases, including 12 warm season and 8 cool season, resulting in a total of 80 model runs. Table 2 lists the physics options used in the LAPS-WRF runs.

Boundary conditions for the WRF runs were obtained from the National Oceanic and Atmospheric Administration (NOAA) Centers for Environmental Prediction (NCEP) North American Mesoscale (NAM) model with a horizontal grid spacing of 12 km. The NAM model domain is on a Lambert conformal projection with a horizontal domain size of 614 by 239 grid points and 42 vertical levels. The NAM model produces an 84-hr forecast every six hours, or four times per day. The NAM model was chosen for boundary conditions as it has the best resolution of all available datasets. Initial conditions for the WRF runs were provided by the LAPS analysis. The background model for the LAPS analysis was a cold-start 3-km WRF model run, initialized at 0600 UTC on each of the candidate days. The cold-start run also used the 12 km NAM model for initial and boundary conditions and it covered the entire Florida peninsula and surrounding coastal waters. This output was then used to create a 1.3 km LAPS analysis at 0900 UTC for each candidate day.

Physics Option	LAPS-WRF
Microphysical scheme	Lin et al. (1983)
Planetary boundary layer scheme	Mellor-Yamada-Janjic (Janjic 1990, 1996, 2002)
Land surface option	Noah Land Surface Model (Chen and Dudhia 2001)
Surface layer scheme	Janjic Eta (Janjic 1996, 2002)
Shortwave radiation scheme	Goddard (Chou and Suarez 1994)
Longwave radiation scheme	RRTM (Mlawer et al. 1997)

The WRF EMS was run as if in real-time. It ingested satellite data in Man computer Interactive Data Access System (McIDAS) Area format 15 minutes prior to the model initialization time; raw, full volume, radar data within 10 minutes of the model initialization time; and surface data from 15 minutes before to 5 minutes after model initialization. The largest task in configuring LAPS was working with the ingest code. This code can only be used with raw data that have the same configuration and format as the NOAA Earth System Research Laboratory Global Systems Division's (GSD) raw data, which is the Network Common Data Form (NetCDF). Therefore, all data files were converted to NetCDF format to be used within LAPS. Software to convert the WSR-88D data and model data to NetCDF format was obtained from GSD. Scripts were written to convert raw wind tower and RAOB data into a format ingestible by LAPS. Two sets of wind tower data were created: one that included all wind tower data from KSC/CCAFS and one that excludes the mainland tower data. Wind tower data from 15 minutes before to 5 minutes after the analysis time were included in the LAPS analysis.

Converting satellite data in McIDAS Area format to NetCDF required several steps. The AMU first ported the data to the local Meteorological Interactive Data Display System (MIDDS) system where they were remapped to the Lambert Conformal projection using the IMGREMAP command. Next, the remapped data were run through a program that converted them to NetCDF format. This program is called AreaToNetCDF and is available from the Space Science and Engineering Center (SSEC) at the University of Wisconsin. All of the reformatted data files were then ingested into LAPS to create an initialization field for the model.

2.5 Problems Encountered

The AMU encountered two problems while using the LAPS software. First, in the most recent LAPS version available at the time of this task, version 0-32-15, an error in the output occurred in which values of rainwater and graupel mixing ratio were set to 0. The AMU determined that the problem might not be able to be remedied within a reasonable amount of time so a previous version of LAPS in which this error did not occur was used instead. Second, the AMU identified a warm bias on the order of 10-15° F in the surface temperature field in all WRF model 0-hr output. The authors contacted Dr. John McGinley of GSD to determine the cause of the problem. After consultation with Dr. McGinley, the bias was traced back to the default bottom pressure level extending below the terrain and the observations. The default bottom pressure levels were 1050 and 1100 mb, corrected to sea level. Dr. McGinley indicated when LAPS has more than one level below the terrain, problems can occur since the software is still applying balance at fictional levels. Assumptions and errors in the extrapolation of pressure to sea level could cause some parts of the lowest levels to be above ground in mountainous Colorado region, where LAPS was originally developed and used. The default pressure levels originally worked since some part of the bottom pressure levels were above ground. Dr. McGinley suggested the best solution for the Florida region was to minimize the value and depth of the lowest pressure level. Hence, the AMU deleted the 1100 mb pressure level and LAPS-WRF was rerun for all candidate days.

3. Analyses

The AMU conducted both subjective and objective analyses of the WRF wind forecasts and compared them to the observed winds at the KSC/CCAFS towers. As stated in the introduction, the AMU was to evaluate the impacts of removing the mainland wind towers and all but one recurring XMR RAOB from the initialization of a local NWP model to determine the impact, if any, to the model forecast. The AMU initialized the WRF model with four different scenarios:

- With the mainland towers and the 1000 UTC XMR RAOB,
- With the mainland towers and without the 1000 UTC XMR RAOB,
- Without the mainland towers and with the 1000 UTC XMR RAOB, and
- Without the mainland towers and without the 1000 UTC XMR RAOB.

In the subjective analysis, the AMU compared the model output of forecast radar reflectivity, peak winds and average winds to the corresponding observations under these four scenarios for the 12 warm season cases and eight cool season cases. For the objective analysis, the AMU identified the model-domain peak wind speed for each forecast output time using the Grid Analysis and Display System (GrADS) software. The model-domain peak wind speed was then compared to the observed maximum peak wind speed in the wind tower network.

3.1 Subjective Wind Analysis

The AMU completed a subjective analysis of the WRF forecasts for all warm season and cool season cases. This was accomplished by creating four-panel images displaying model output and observations at the time of the maximum peak wind corresponding to the 45 WS warnings and advisories for that day. The model output was compared to the observations to determine if any of the four scenarios produced better results than the others. The goals were to determine if the model could provide an indicator to the forecaster that there may be winds meeting advisory or warning criteria for the day and if excluding mainland wind towers and/or the XMR RAOB made a difference in the model wind forecast. One case from the warm season and one from the cool season are discussed in this section.

3.1.1 Warm Season

During the warm season, WRF peak wind forecasts were highly correlated with the location and strength of the forecast radar reflectivity and, therefore, was the one model parameter assessed besides winds. On 20 June 2007, the 45 WS issued a Weather Watch for winds ≥ 50 kt, hail ≥ 0.75 in and/or tornadoes valid from 1830 to 2000 UTC. They then issued a Wind Warning for winds from the surface to 300 ft ≥ 35 kt for KSC after a peak wind of 38 kt was observed at 2115 UTC on Tower 421 at the north end of KSC. For this event, the 45 WS had -49 minutes lead time and -75 minute timing error (i.e., the warning was issued after the event occurred and the event occurred after the watch had expired). The observed wind gust was generated by an isolated thunderstorm and was the only one that met the warning criteria that day. .

The AMU first compared the 12-hr model forecast radar reflectivity (valid at 2100 UTC) to 2117 UTC observed radar reflectivity from the Melbourne, FL WSR-88D. As shown in Figure 3, the model forecast radar reflectivity in all four scenarios did a fairly good job depicting the observed broken line of convection extending northeast to southwest from offshore northern KSC and across the mainland. For this event, the scenarios that included the mainland towers and the RAOB (Figure 3b) and excluded the mainland towers and included the RAOB (Figure 3d) best matched the observed radar reflectivity in coverage, location and intensity. It is also interesting to note the two best scenarios occurred both with and without mainland wind tower data. However, there was little difference among all four scenarios, which raises the question, "Would any of the forecasts have helped the forecaster issue a better watch or warning?"

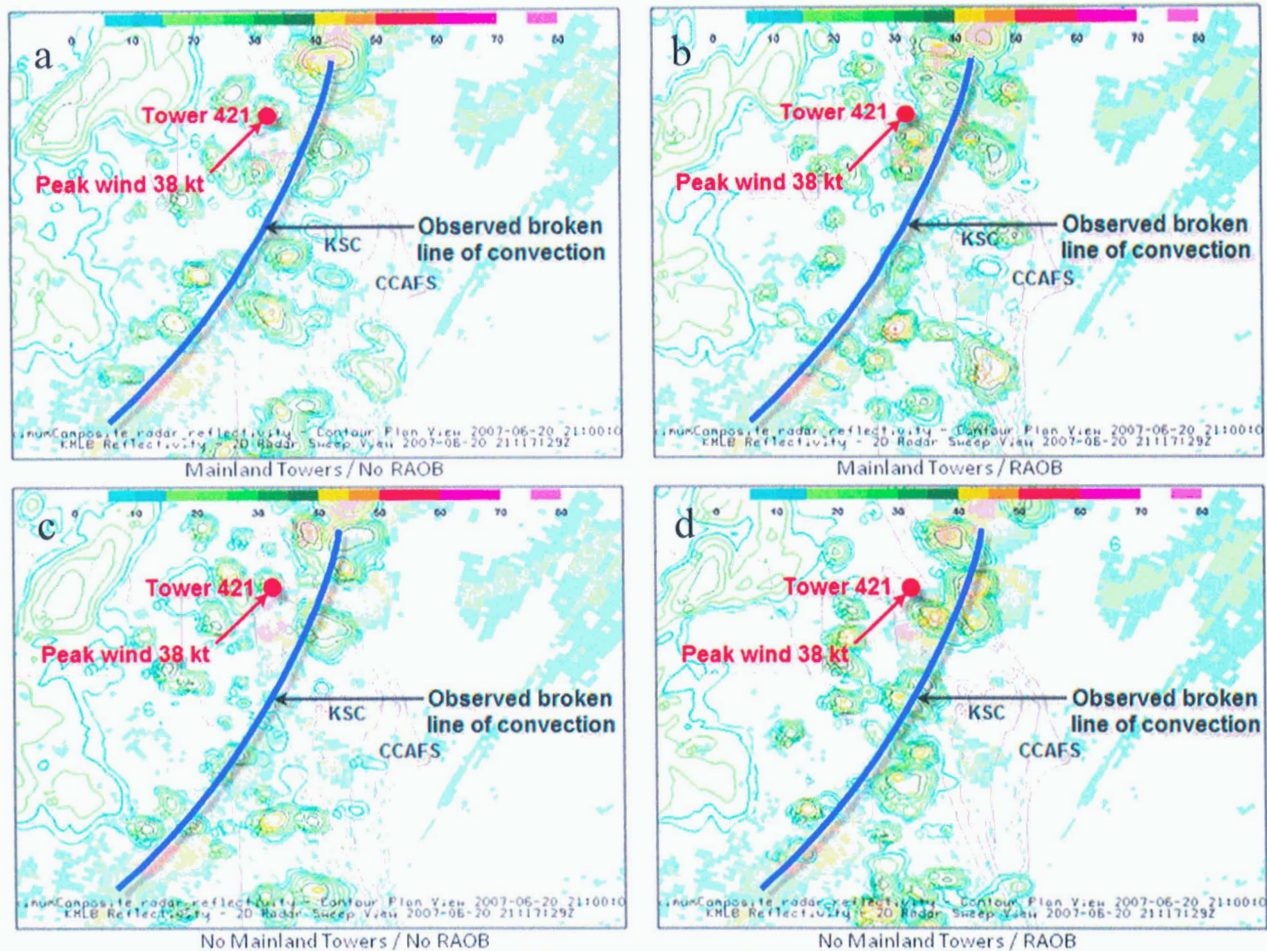


Figure 3. Comparison of the 2100 UTC model forecast radar reflectivity (contours) to the 2117 UTC observed radar reflectivity from the NWS MLB WSR-88D (shaded) for the four scenarios on 20 June 2007. The model forecast radar reflectivity contours based on (a) the mainland towers and no RAOB , (b) mainland towers with the RAOB , (c) no mainland towers and no RAOB and (d) no mainland towers with RAOB . The reflectivity scale (dBZ) is shown at the top of each map. The location of the maximum peak wind speed is shown at Tower 421 by the red dot. The approximate broken line of observed convection is shown in blue.

The AMU compared the 12-hr model forecast peak wind speeds valid at 2100 UTC to the 2115 UTC observed peak winds from the KSC/CCAFS towers as shown in Figure 4. In all four scenarios the maximum peak winds were highly correlated to the model forecast radar reflectivity. The scenarios that included the mainland towers and the RAOB (Figure 4b) and excluded the mainland towers and included the RAOB (Figure 4d) best matched the observed peak winds in location and speed. As with the forecast radar reflectivity, there was little difference among all four scenarios. Any one of the four model runs would have given the forecaster an indication to expect convective winds in the 25-30 kt range during the day. Although the model did not forecast peak winds at or above the warning threshold, the output provided valuable information that would have allowed the forecaster to be alert for convective winds requiring a warning.

The AMU also compared the model forecast average wind speeds to the KSC/CCAFS towers for each warm season case as was done for the peak wind speeds. The model forecast average wind speeds aligned well with the model forecast peak wind speeds in location and relative speed. Since every warm season wind event was convective in nature, the model forecast average speeds did not provide any additional information of value and, therefore, are not discussed here.

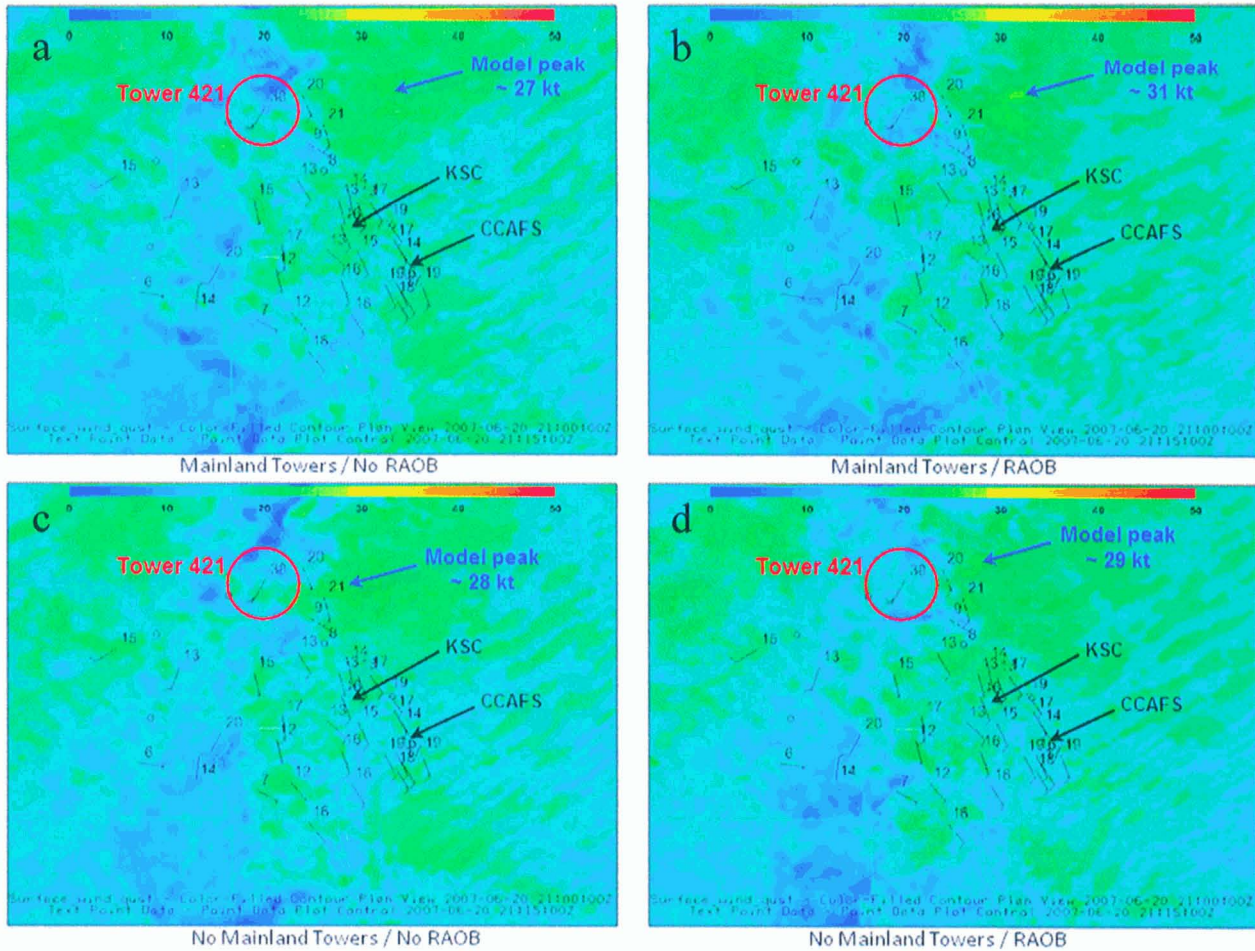


Figure 4. Comparison of the 2100 UTC model forecast peak winds (shaded) to the 2115 UTC wind tower observations for the four scenarios of data withholding on 20 June 2007. The wind tower observations show the 5 minute average wind speed and direction (wind barb) and peak speed (number at upper right of the wind barb). The model forecast peak wind speeds based on the (a) mainland towers and no RAOB , (b) mainland towers with the RAOB , (c) no mainland towers and no RAOB and (d) no mainland towers with RAOB . The model wind speed scale (kt) is shown at the top of each map. The location of the maximum peak wind speed is shown at Tower 421 by the red circle.

3.1.2 Cool Season

During the cool season, synoptic scale gradient flow was the primary cause of high wind events that warranted 45 WS advisories and warnings. None of the cool season cases were associated with convection. Based on the subjective analysis, the WRF peak wind speed forecasts were better during the cool season in both timing and location compared with the warm season forecasts which is expected as the model can better handle strong synoptic scale forcing vs. weak mesoscale forcing. On 17 January 2008, the 45 WS issued a Wind Warning for winds from the surface to 300 ft \geq 50 kt for KSC valid from 1200 to 1700 UTC. It was downgraded to a Wind Warning for winds from the surface to 300 ft \geq 35 kt for KSC at 1612 UTC after observing a maximum peak of 33 kt at Tower 313 at 1500 UTC. Figure 5 shows the WRF peak wind speed forecast (shaded) at \sim 33 ft at 1500 UTC with a plot of the observed winds at 54 ft from the KSC/CCAFS mesonet towers and 295 ft from Tower 313 at 1500 UTC. The WRF forecast of peak winds indicated they would be stronger over KSC/CCAFS and offshore than inland with peak speeds of \sim 20-25 kts inland, increasing to \sim 27-31 kts along the coast, and then $>$ 35 kt offshore. The observed winds were lower than forecast, but the trend was the same with the strongest winds at the coastal towers. As with the warm season cases, there was little difference among all four model runs in this case as well as the other seven cool season cases. Any one of the four model runs would have given the forecaster an indication to expect peak winds in the 30-35 kt range during the day with the strongest winds closer to the coast.

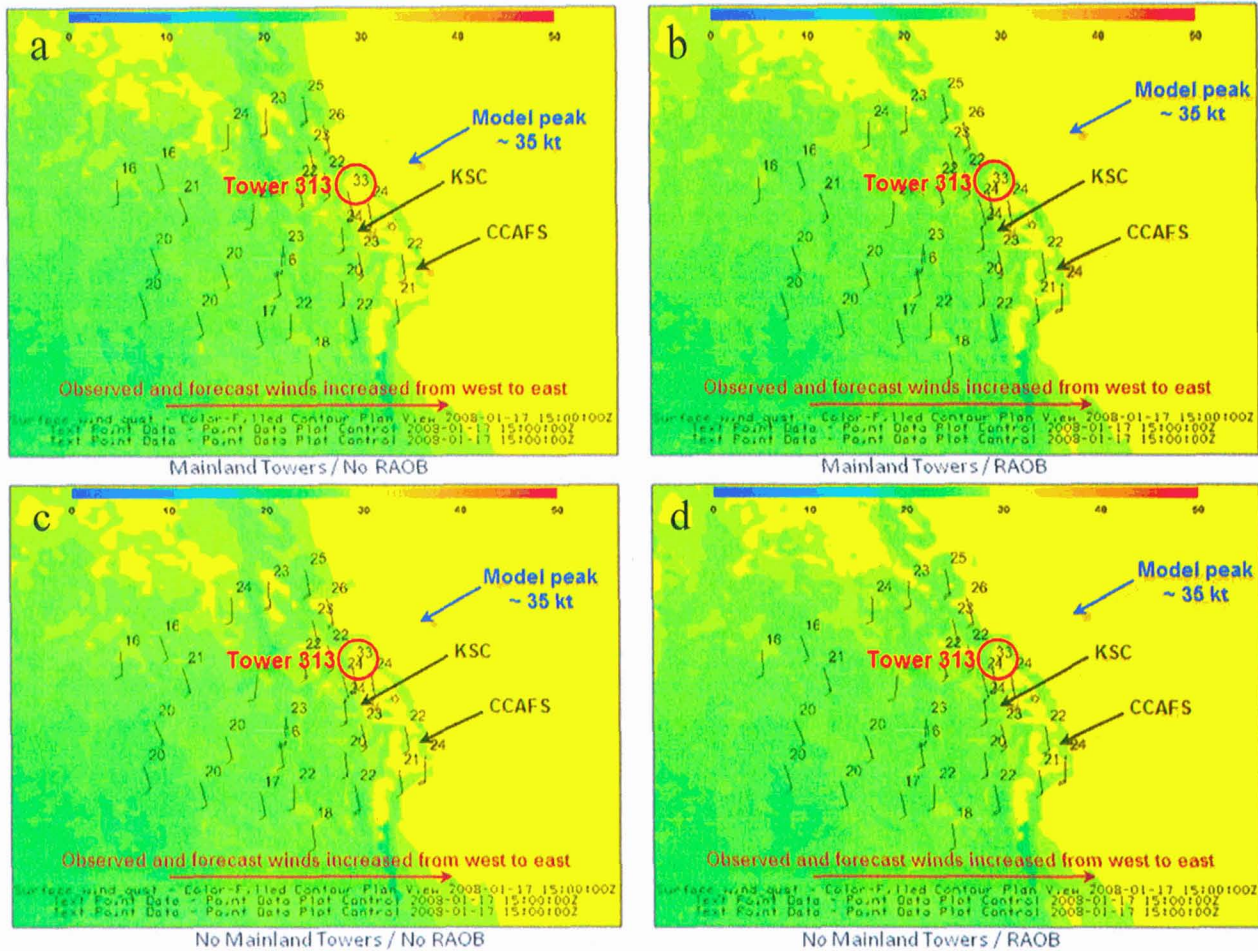


Figure 5. Comparison of the model forecast peak winds (shaded) to the wind tower observations for the four scenarios of data withholding on 17 January 2008 at 1500 UTC. The wind tower observations show the 5 minute average wind speed and direction (wind barb) and peak speed (number at upper right of the wind barb). The model forecast peak wind speeds based on the (a) mainland towers and no RAOB , (b) mainland towers with the RAOB , (c) no mainland towers and no RAOB and (d) no mainland towers with RAOB . The model wind speed scale (kt) is shown at the top of each map. The location of the maximum peak wind speed is shown at Tower 313 by the red circle.

The AMU also compared the model forecast average wind speeds for each cool season case to the KSC/CCAFS towers. As stated previously, none of the cool season cases were associated with convection and based on the subjective analysis. Like the WRF peak wind speed forecasts, the WRF average wind speed forecasts were better during the cool season in both timing and location compared with the warm season forecasts. Figure 6 shows the WRF average wind speed forecast (shaded) at ~ 33 ft at 1500 UTC 17 January 2008 with a plot of the observed average wind speeds at 54 ft from the KSC/CCAFS mesonet towers and 295 ft from Tower 313 at 1500 UTC. Like the WRF forecast of peak wind speeds for this case, the WRF forecast of average wind speeds indicated they would be stronger over KSC/CCAFS and offshore than inland with speeds of ~ 13-18 kts inland, increasing to ~ 18-24 kts along the coast, and then > 25 kt offshore. The observed winds were lower than forecast, but the trend was the same with the strongest winds at the coastal towers. As with the warm season cases, there was little difference among all four scenarios in this case as well as the other seven cool season cases. Any one of the four model runs would have given the forecaster an indication to expect sustained winds in the 18-24 kt range during the day with the strongest winds closer to the coast.

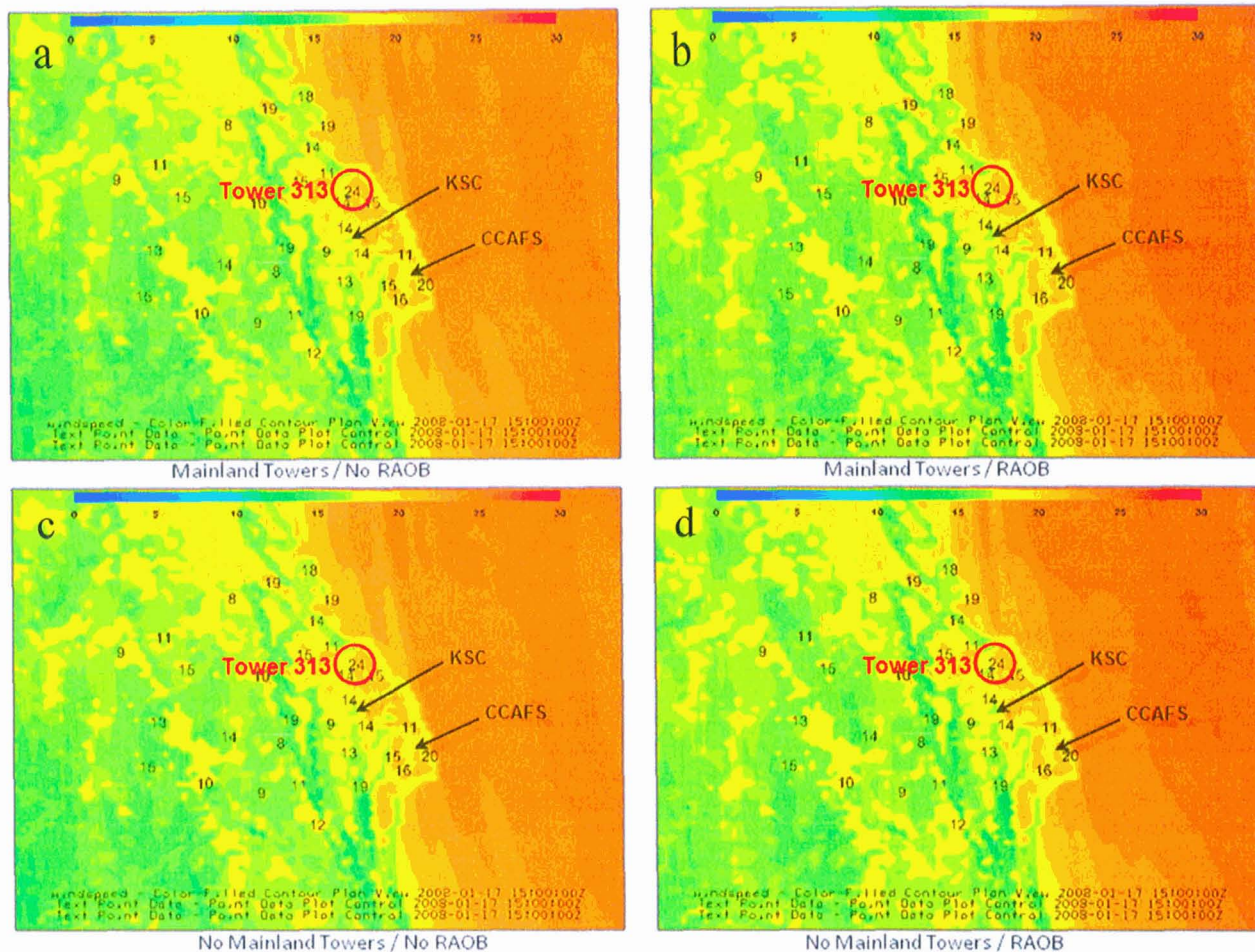


Figure 6. Comparison of the model forecast average winds (shaded) to the wind tower observations for the four scenarios of data withholding on 17 January 2008 at 1500 UTC. The model forecast average wind speeds based on the (a) mainland towers and no RAOB, (b) mainland towers with the RAOB, (c) no mainland towers and no RAOB and (d) no mainland towers with RAOB. The black numbers are the 5 minute average wind speed observations at 54 ft. The location of the highest average wind speed is shown at Tower 313 by the red circle. The model wind speed scale (kt) is shown at the top of each map.

3.2 Objective Peak Wind Analysis

Upon reviewing the results of the subjective analysis, the 45 WS asked the AMU to conduct an objective analysis of the peak wind comparisons. To do this, the AMU identified the maximum model-domain peak wind speed for each forecast output time using GrADS. The *max()* function in GrADS allows the user to identify the maximum value of a variable within a user specified domain. This function was used to return the maximum peak wind speed within the domain pictured in Figure 7. Using the results from GrADS, the AMU compared the WRF forecast maximum peak wind speed to the observed maximum peak wind speed and then conducted an overall evaluation of how well the four model scenarios performed against each other.

An example of the objective analysis output from a warm season case on 11 July 2007 is shown by the chart in Figure 8. The maximum observed wind speed and the model forecast maximum wind speed for the four scenarios are plotted over the 12-hr forecast period at 60-minute intervals. All four model runs were consistent with each other and forecast a steady to decreasing maximum peak wind speed between the 0- and 5-hr forecasts, and then an increase from the 5- to the 10-hr forecast followed by a decreasing trend. The model forecasts matched the trend of the observed maximum peak wind speed in the domain. The average difference between the lowest and highest forecast maximum peak wind speeds in the four WRF runs for all 12 hr output intervals was 1.79 kt. The average mean squared error (MSE) between the average of the four WRF forecasts and observed maximum peak wind

speeds was 4.91 kt. The largest MSE of 19.67 kt occurred at the 12 hr WRF forecast interval. The observed maximum peak wind speed of 31 kt was associated with a convective thunderstorm gust.

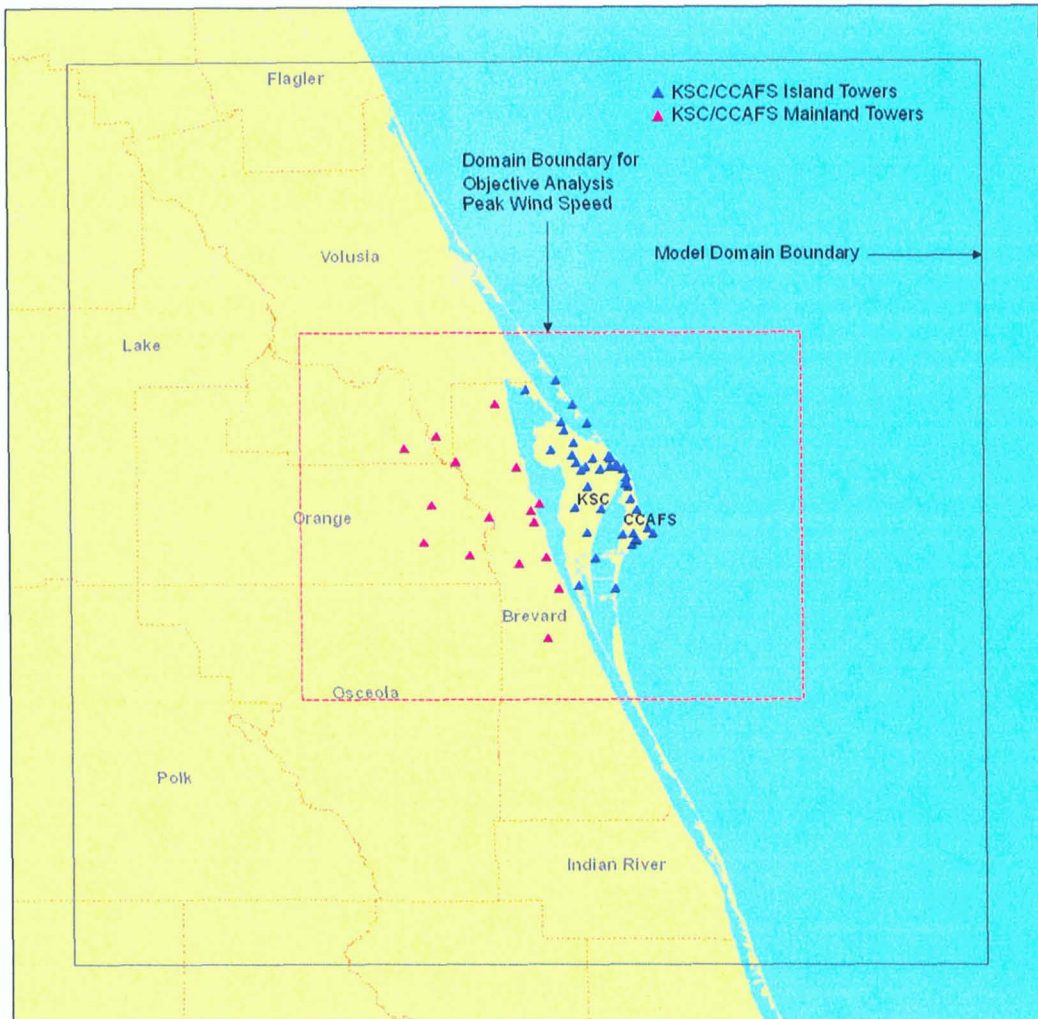


Figure 7. Map of east-central Florida showing the location of the model sub-domain, outlined by the red-dashed rectangle, used in the objective analysis portion of this task.

An example of the objective analysis output from a cool season case on 11 January 2008 is shown by the chart in Figure 9. The maximum observed wind speed and the model forecast maximum wind speed for the four scenarios are plotted over the 12-hr forecast period at 30-minute intervals. As with the warm season case, all four model runs were consistent with each other. The WRF forecasts predicted an increasing trend in the maximum peak wind speeds from the 0- to 2.5-hr forecast, and then a steady to decreasing trend from the 2.5- to 12-hr forecast. The model forecasts matched the trend of the observed maximum peak wind speed in the domain. The average difference between the lowest and highest forecast maximum peak wind speeds in the four WRF runs for all 12 hr output intervals was 1.68 kt. The average mean square error (MSE) between the average of the four WRF forecasts and observed maximum peak wind speeds was 4.49 kt. The largest MSE of 11.25 kt occurred at the 0-hr forecast interval. The observed maximum peak wind speed of 43 kt occurred at the 2-hr forecast interval. It is interesting to note that one of the WRF forecasts predicted a maximum peak wind speed of 41.4 kt 30 minutes after the observed maximum peak wind speed of 43 kt indicating the model did an excellent job forecasting the magnitude of the maximum peak wind speed with timing being only slightly off.

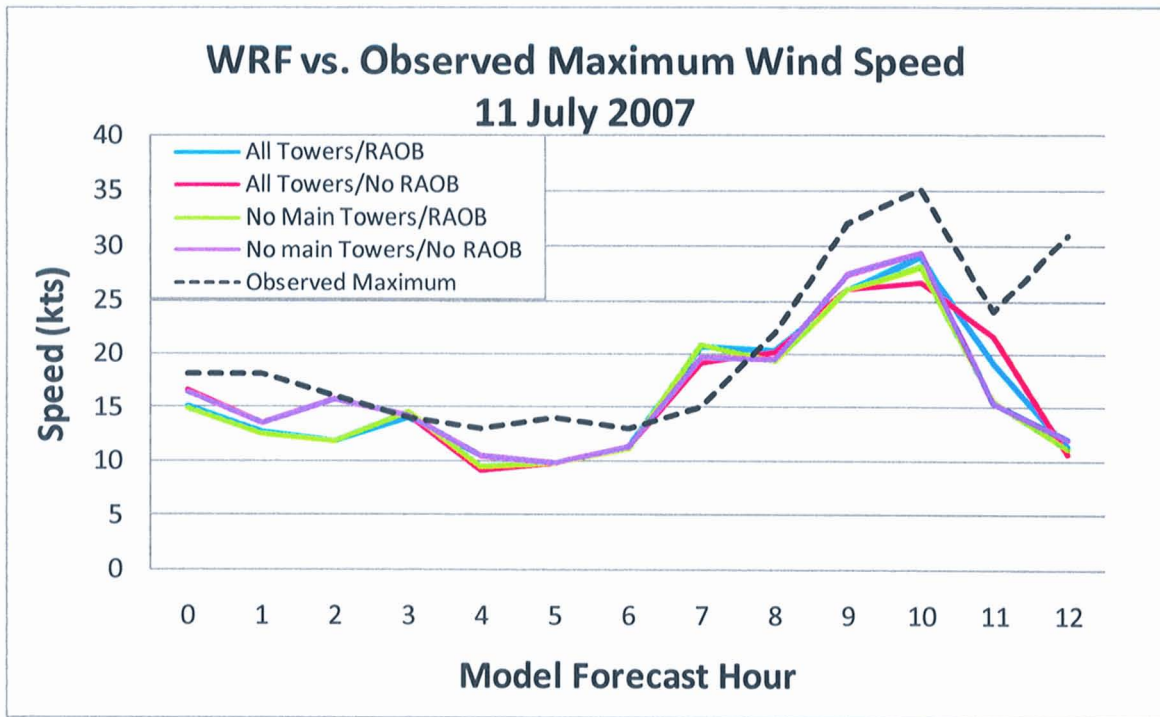


Figure 8. Chart of the observed maximum wind speed from the KSC/CCAFS towers and the model forecast maximum peak wind speed for the four scenarios on 11 July 2007 for all 12 1-hour forecast periods.

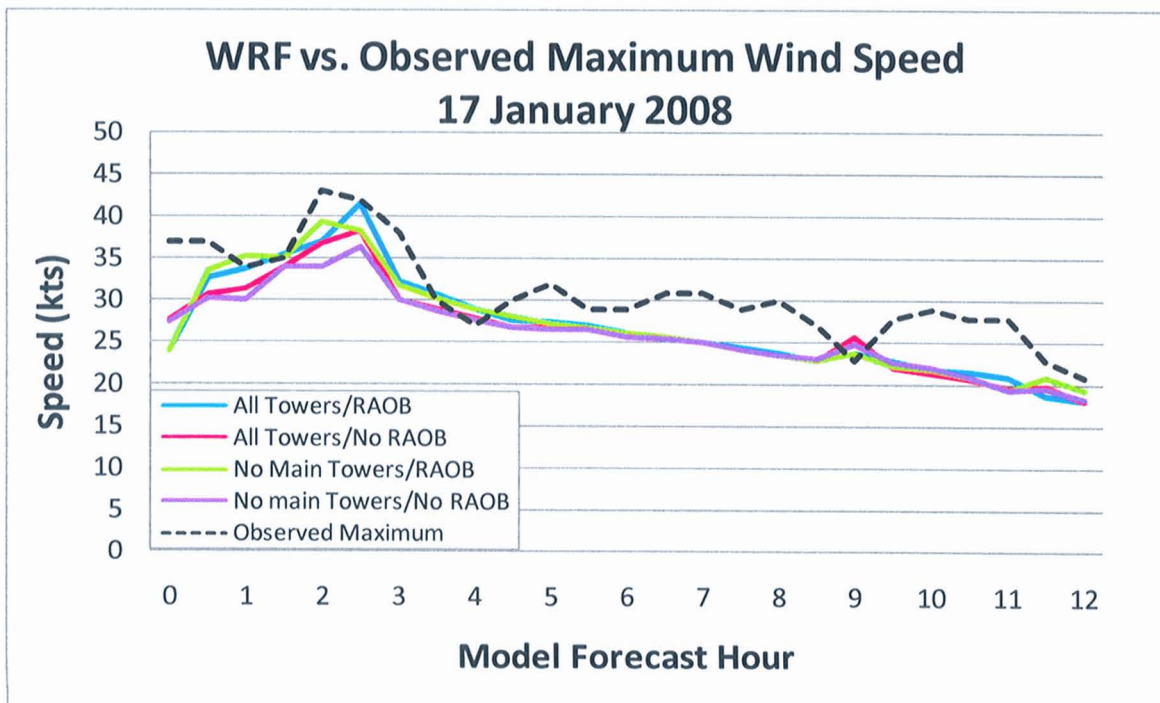


Figure 9. Chart of the observed maximum wind speed from the KSC/CCAFS towers and the model forecast maximum peak wind speed for the four scenarios on 17 January 2008 for all 24 30-minute forecast periods.

After comparing the WRF maximum peak wind speed forecasts to the observed maximum peak wind speed, the AMU computed statistics for the overall model performance for all 20 cases. The first question to answer was whether or not any one of the four scenarios performed better than the other three with regard to the maximum peak wind forecasts. To do this, the AMU computed the average difference between the maximum and minimum WRF forecast for each forecast hour in each case. The results are shown in Table 3. During the warm season, the four scenarios were within 2 kt of each other through the 7-hr forecast interval and then diverged. The cool season results indicate the four scenarios tracked better after the 4-hr forecast interval and remained within 1.4 kt of each other. The data from Table 3 is shown in the chart in Figure 10. Overall, the average difference in the four WRF scenarios for the entire 12-hr forecast period was 1.91 kt for the warm season and 1.38 kt for the cool season. This indicates the data denial scenarios performed comparably to the data rich scenarios.

Table 3. Differences in the WRF maximum peak wind speed forecasts among the four “with and without” data scenarios for all of the warm season and cool season cases for each forecast hour of the model.			
Warm Season		Cool Season	
WRF Forecast Hour	Avg Difference Among the Four Scenarios (kt)	WRF Forecast Hour	Avg Difference Among the Four Scenarios (kt)
0	1.05	0	1.08
1	1.44	1	1.89
2	1.83	2	2.09
3	1.59	3	2.63
4	1.19	4	1.25
5	1.30	5	1.38
6	1.10	6	1.22
7	1.94	7	1.04
8	2.72	8	1.15
9	2.46	9	1.14
10	2.43	10	0.87
11	3.27	11	1.11
12	2.51	12	1.08

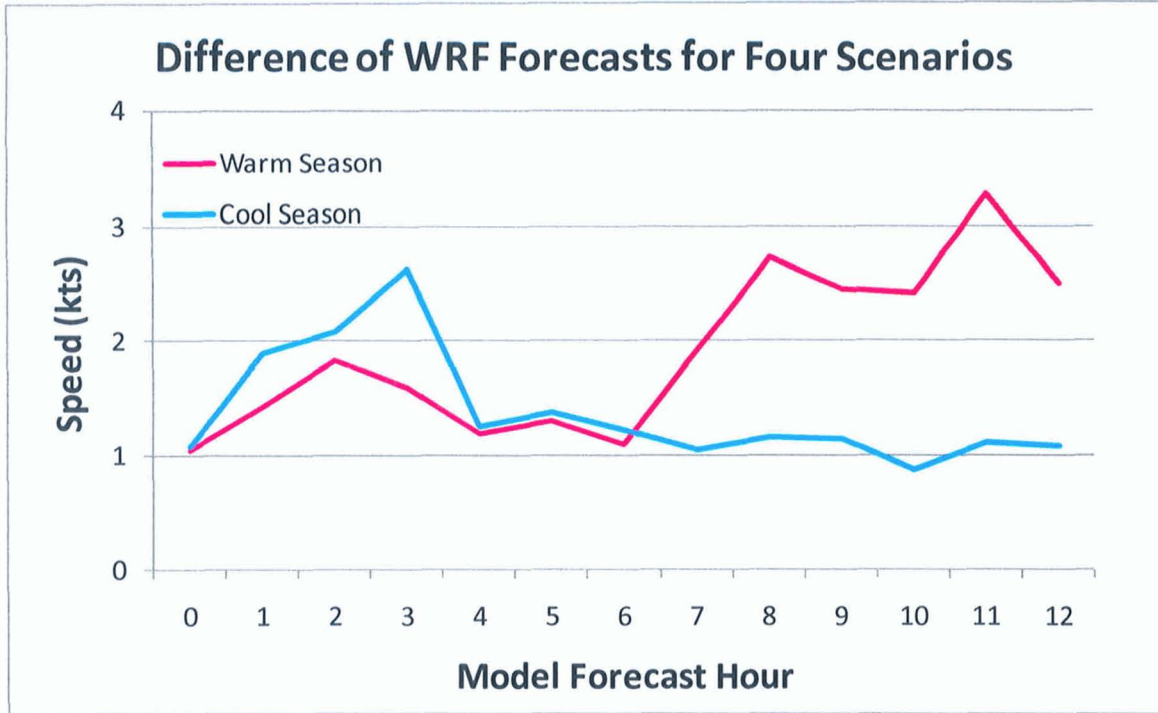


Figure 10. Chart showing the differences in WRF forecasts of maximum peak wind speed among the four scenarios for each hour of the model forecast for both the warm season (red line) and cool season (blue line).

Finally, the AMU computed the RMSE using the equations below for all cases to compare the WRF forecasts to the observed maximum peak wind speeds. The results are shown in Table 4 and the corresponding chart is shown in Figure 11.

$$MSE = \frac{1}{n} \sum_{i=1}^n (f_i - o_i)^2$$

$$RMSE = \sqrt{MSE}$$

Where:

$n = 12$ for the warm season and 8 for the cool season,

f = average of four WRF forecast scenario maximum peak wind speeds for each WRF forecast interval, and

o = average of the observed maximum peak wind speeds for each WRF forecast interval.

During the warm season, the WRF RMSE decreased from the 0- to the 3-hr forecast by just over 2 kt and then generally increased throughout the 12-hr forecast period to a maximum RMSE of 13.87 kt at the 11-hr forecast. During the cool season, the WRF RMSE was consistent throughout most of the forecast intervals at about 5-7 kt with a maximum RMSE of 7.77 kt at the 2-hr forecast. This data indicates WRF performance is worse in the warm season over the sub-domain.

The MSE provides an overall indication of model performance for the cases investigated in this work. However, on certain days the MSE was as large as 30 kt during the warm season and 16 kt during the cool season. Sometimes the error was due to WRF incorrectly forecasting the magnitude of the peak wind speed for the day while at other times WRF forecast the magnitude correctly but error was due to timing. The bias of the model compared to the observations for the warm season was -3.27 kt and for the cool season -3.40 kt. This indicates a tendency for WRF to under forecast peak wind events in both seasons.

Table 4. The RMSE of the WRF maximum peak wind speed forecasts among the four “with and without” data scenarios compared to the observations for all of the warm season and cool season cases for each forecast hour of the model.

Warm Season		Cool Season	
WRF Forecast Hour	RMSE (kt)	WRF Forecast Hour	RMSE (kt)
0	4.71	0	5.93
1	3.45	1	6.33
2	3.34	2	7.77
3	2.33	3	5.68
4	6.27	4	7.04
5	7.17	5	5.69
6	4.82	6	5.05
7	7.35	7	4.36
8	7.75	8	5.21
9	9.56	9	4.75
10	9.23	10	6.13
11	13.87	11	5.82
12	10.89	12	4.97

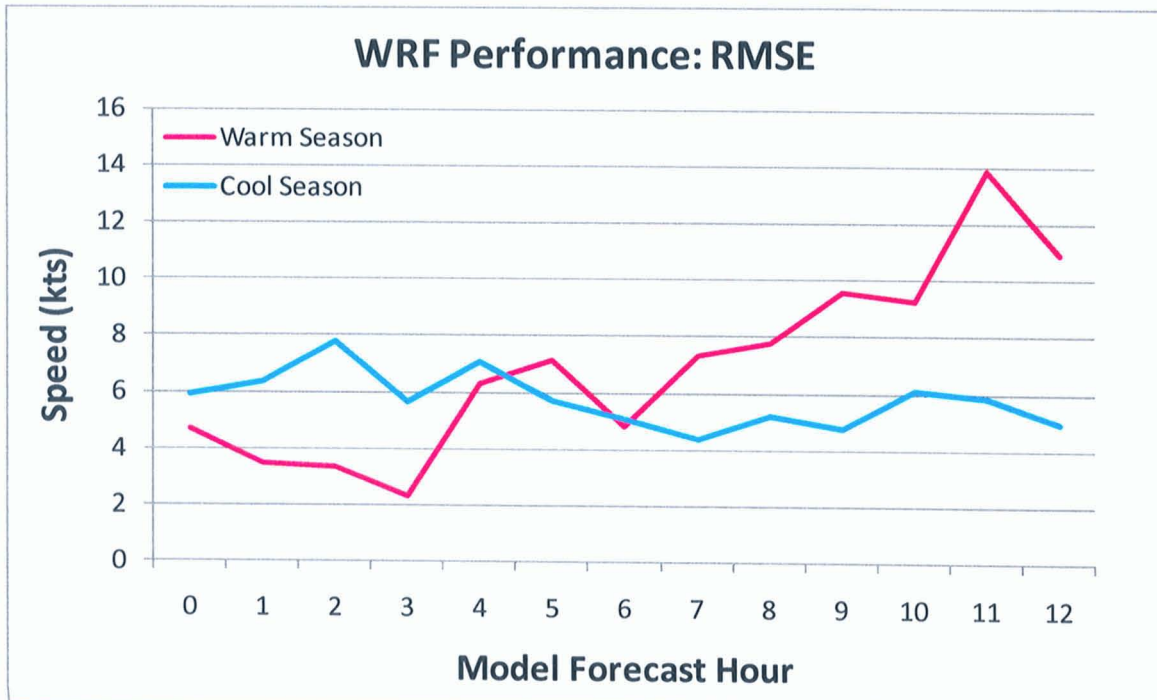


Figure 11. Chart showing the RMSE among the four WRF forecasts of maximum peak wind speed and the observations for each hour of the model forecast for both the warm season (red line) and cool season (blue line).

4. Summary and Conclusions

The 45 WS forecasters use observations from the KSC/CCAFS wind tower network and the XMR RAOB to issue and verify wind advisories and warnings for operations. SMG and NWS MLB use these observations to initialize their locally-run mesoscale models, and SMG also uses them to support shuttle landings at the SLF. Due to impending budget cuts, some or all of the KSC/CCAFS wind towers on the east-central Florida mainland and some XMR RAOBs may be eliminated. The loss of these data may impact the forecast capability of the 45 WS, SMG and NWS MLB.

The AMU conducted a modeling study to determine how important these observations are to the accuracy of the model output used by the forecasters as input to their forecasts. This study was done in two steps: 1) Initializing the WRF model with and without KSC/CCAFS wind tower and XMR RAOB data, and 2) Assessing the accuracy of model output by comparing peak wind forecasts to observations meeting wind advisory and warning criteria as forecast by the 45 WS.

To keep the study manageable yet representative of the weather in different seasons, the AMU collected data for 12 warm season cases from June – September 2007 and eight cool season cases from November – January 2008. To keep the study focused, the AMU chose only cases in which the 45 WS issued a wind advisory or warning for the KSC/CCAFS area and the KSC/CCAFS wind towers recorded significant wind events, i.e. winds greater than 18 kt.

The AMU used the WRF model with a “hot-start” initialization using LAPS. Each run started at 0900 UTC and was integrated 12 hours with a 1.3 km horizontal grid spacing and 40 irregularly spaced, vertical sigma levels. Data used to initialize LAPS included Level II WSR-88D data from the NWS MLB radar, GOES visible and infrared satellite imagery, MADIS data, and KSC/CCAFS wind tower data and the XMR RAOB. The AMU initialized LAPS using four different combinations of the local data in question:

- With the mainland towers and without the 1000 UTC XMR RAOB,
- With the mainland towers and with the 1000 UTC XMR RAOB,
- Without the mainland towers and without the 1000 UTC XMR RAOB, and
- Without the mainland towers and with the 1000 UTC XMR RAOB.

The AMU conducted a subjective analysis of the WRF forecasts by comparing model output to observations at the time of the maximum peak wind corresponding to the 45 WS advisories and warnings to determine if any of the four scenarios produced better results than the others. A two-part objective analysis was also conducted. In the first part, the model-domain maximum peak wind speeds for each forecast output time were compared to the observed maximum peak wind speed in the domain. The second part incorporated evaluating how well the four model scenarios performed against each other.

In both the subjective and objective analyses, the AMU found little difference among the four WRF model scenarios. The WRF model did perform better in the cool season during prevailing synoptic forcing regimes and it was also a good indicator of the threat of advisory or warning criteria wind speeds over each 12-hr forecast model run. This would provide added value to the forecaster’s daily planning forecast.

References

- Albers, S. C., 1995: The LAPS wind analysis. *Wea. Forecasting*, **10**, 342–352.
- Albers, S. C., J. A. McGinley, D. L. Birkenheuer, and J. R. Smart, 1996: The Local Analysis and Prediction System (LAPS): Analyses of clouds, precipitation, and temperature. *Wea. Forecasting*, **11**, 273–287.
- Birkenheuer, D., 1999: The effect of using digital satellite imagery in the LAPS moisture analysis. *Wea. Forecasting*, **14**, 782–788.
- Chen, F., and J. Dudhia, 2001: Coupling an advanced land-surface/ hydrology model with the Penn State/ NCAR MM5 modeling system. Part I: Model description and implementation. *Mon. Wea. Rev.*, **129**, 569–585.
- Chou M.-D., and M. J. Suarez, 1994: An efficient thermal infrared radiation parameterization for use in general circulation models. NASA Tech. Memo. 104606, 3, 85pp.
- Fulton, R. A., J. P. Breidenbach, D. Seo, D. A. Miller, T. O'Bannon, 1998: The WSR-88D rainfall algorithm. *Wea. Forecasting*, **13**, 377-395.
- Janjic, Z. I., 1990: The step-mountain coordinate: physical package, *Mon. Wea. Rev.*, **118**, 1429–1443.
- Janjic, Z. I., 1996: The surface layer in the NCEP Eta Model. 11th Conf. on Numerical Weather Prediction, Norfolk, VA, 19–23 August, Amer. Meteor. Soc., Boston, MA, 354–355.
- Janjic, Z. I., 2002: Nonsingular Implementation of the Mellor–Yamada Level 2.5 Scheme in the NCEP Meso model, NCEP Office Note, No. 437, 61 pp.
- Lin, Y.-L., R. D. Farley, and H. D. Orville, 1983: Bulk parameterization of the snow field in a cloud model. *J. Climate Appl. Meteor.*, **22**, 1065–1092.
- McGinley, J. A., 1995: Opportunities for high resolution data analysis, prediction, and product dissemination within the local weather office. 14th Conf. on Weather Analysis and Forecasting, Dallas, TX, Amer. Meteor. Soc., 478-485.
- McGinley, J. A., S. C. Albers, and P. A. Stamus, 1991: Validation of a composite convective index as defined by a real-time local analysis system. *Wea. Forecasting*, **6**, 337–356.
- Mlawer, E. J., S. J. Taubman, P. D. Brown, M. J. Iacono, and S. A. Clough, 1997: Radiative transfer for inhomogeneous atmosphere: RRTM, a validated correlated-k model for the longwave. *J. Geophys. Res.*, **102** (D14), 16663–16682.
- Rozulmalski, R., 2006: WRF Environmental Modeling System User's Guide. NOAA/NWS SOO Science and Training Resource Coordinator Forecast Decision Training Branch, 89 pp. [Available from COMET/UCAR, P.O. Box 3000, Boulder, CO, 80307-3000].
- Skamarock, W. C., J. B. Klemp, J. Dudhia, D. O. Gill, D. M. Barker, W. Wang, and J. G. Powers, 2005: A description of the Advanced Research WRF Version 2. NCAR Technical Note NCAR/TN-468+STR, 88 pp.

List of Acronyms

45 WS	45th Weather Squadron	NAM	North American Mesoscale model
AMU	Applied Meteorology Unit	NCEP	National Centers for Environmental Prediction
CCAFS	Cape Canaveral Air Force Station	NetCDF	Network Common Data Form
GrADS	Grid Analysis and Display System	NOAA	National Oceanic and Atmospheric Administration
GOES	Geostationary Operational Environmental Satellites	NWS	National Weather Service
GSD	Global Systems Division	POR	Period of Record
KSC	Kennedy Space Center	RAOB	Rawinsonde observation
LAPS	Local Analysis and Prediction System	SLF	Shuttle Landing Facility
MADIS	Meteorological Assimilation Data Ingest System	SMG	Spaceflight Meteorology Group
McIDAS	Man computer Interactive Data Access System	SSEC	Space Science and Engineering Center
MIDDS	Meteorological Interactive Data Display System	WRF	Weather Research and Forecasting model
MSE	Mean Square Error	WSR-88D	Weather Surveillance Radar-1988 Doppler
		XMR	CCAFS rawinsonde 3-letter identifier

NOTICE

Mention of a copyrighted, trademarked or proprietary product, service, or document does not constitute endorsement thereof by the author, ENSCO Inc., the AMU, the National Aeronautics and Space Administration, or the United States Government. Any such mention is solely for the purpose of fully informing the reader of the resources used to conduct the work reported herein.